

Article

Influence of Surface Reflection (Albedo) in Simulating the Sun Drying of Paddy Rice

Ana Salvatierra-Rojas * , Victor Torres-Toledo and Joachim Müller 

Institute of Agricultural Engineering, Tropics and Subtropics Group (440e), University of Hohenheim, 70599 Stuttgart, Germany; victor.torrestoledo@uni-hohenheim.de (V.T.-T.); joachim.mueller@uni-hohenheim.de (J.M.)

* Correspondence: Ana.SalvatierraRojas@uni-hohenheim.de or info440e@uni-hohenheim.de

Received: 30 June 2020; Accepted: 22 July 2020; Published: 24 July 2020



Abstract: The sun drying of agricultural products is a complicated process involving heat transfer, mass transfer, and variable weather conditions. Surface reflection (albedo), a crop's radiative property, plays an essential role in energy balance, and understanding its contribution can improve the thermal analysis. In this study, field experiments were conducted in the Philippines to explore the influence of surface albedo on the sun drying of paddy rice. First, we implemented energy and mass balance equations in a transient model with the surroundings using a graphical programming language in Matlab/Simulink[®]. Second, we identified the influence of albedo on the sun drying model by using a sensitivity analysis. Third, we investigated the relationship of paddy rice albedo and the solar zenith angle. Lastly, we integrated the albedo function into the sun drying model. The simulation outputs were validated with field experiments. A better estimation of the measured exit temperature and instantaneous mass were obtained when a variable albedo was applied. This study makes clear that introducing a variable albedo has a positive impact on model improvement. This information is important for application in solar drying technologies, so that the drying process can be better assessed.

Keywords: solar energy; thermal analysis; sun drying; paddy rice; albedo; dynamic modeling

1. Introduction

The sun drying of paddy rice is a common practice in the Philippines and many other countries in the tropics and subtropics. Immediately after harvesting/threshing, paddy rice is spread over mats positioned alongside roads or on other paved ground when weather conditions are favorable. To ensure an optimum milling process, it is recommended to dry the paddy rice to a moisture content (MC) of around 14% wet basis [1,2]. During the dry season, the grain temperature can reach up to 55 °C due to the direct exposure of the paddy rice to high solar radiation. Under these conditions, the paddy rice can reach a very low MC (<10% wet basis) [3,4], which may result in fissured grains after milling, thus decreasing its market value. However, during the rainy season, the lower radiation and extended rainy periods may lead to a prolonged drying process. This delay in drying increases the risk of paddy rice deterioration. This deterioration of paddy rice can be observed in the milled rice.

The sun drying of paddy rice is a complex process, which involves the removal of water through direct exposure of the crop to solar radiation. Heat is transferred from the surroundings and from the sun to the exposed crop surface. Raising the crop temperature helps to diffuse water vapor from the interior of the kernel to the surface. Hence, mathematical models have been developed to understand and predict the sun drying process of different agricultural products. Jain and Tiwari [5] proposed the calculation of the convective heat transfer coefficient (h_c), followed by the generation of a mathematical model for the estimation of the crop temperature (T_{crop}) and moisture evaporated (m_{ev}). To simplify the model's solution, a steady state condition is commonly used, and indeed several authors follow

this methodology [6–9]. Even though meteorological conditions have a strong influence on the solar radiation incident on the crop surface, constant radiative properties, such as the reflectivity and absorptivity of the crop, are commonly assumed during the modeling of the sun drying of medicinal plants, cereals, vegetables, and fruits.

A fraction of the incident solar radiation is partly absorbed and scattered by the atmosphere and the earth's different surfaces. Here, the surface reflection (albedo) is the ratio of the reflected solar radiation to the incoming solar radiation [10,11]. Albedo plays a crucial role in the fraction of solar energy absorbed and is a fundamental parameter applied in different research fields, including agriculture, climatology, forestry, building energy, and photovoltaics [12–15]. Previous studies have explored the parametrization of albedo, and most of them reported a close relationship with the solar zenith angle [16–19]. The parametrization of albedo has commonly been used for the improvement of the accuracy of models such as land, weather, and climate forecast models [20].

In rice production, several studies have assessed albedo measurements during the whole cropping period, and some even monitored it up until the harvesting stage. The values ranged from 0.09 to 0.25 [10,21–30]. This information is commonly used for the estimation of surface energy, water budget, and potential cropping yield. However, limited research on albedo in the postharvest processes was found, particularly in the sun drying of paddy rice, where solar energy plays a critical role in the success of drying. Belessiotis and Delyannis [31] suggest albedo values depending on the surface color of the product: dark-colored materials have an albedo value of 0.10, while gray, red, and green materials have a value about 0.30, and light-colored materials have a surface value of about 0.50. For brown rice, Arnize [21] and Bala [32] proposed an albedo value of 0.16.

Three general procedures for measuring albedo can be found in the literature: Laboratory measurements, remotely sensed measurements, and field measurements. First, the laboratory measurements comprise the use of spectral radiometers and solar simulators to measure the spectral reflectivity of small samples; more extensive measurements can be carried out remotely by fixing the spectral radiometer on aircraft or satellites [33]. The second measurement is the remote sensing technique, which provides spectral data that can generate essential information. However, this technique might not be practical for field applications as it requires a careful estimation of atmospheric attenuation and has limited accuracy for small test surfaces in heterogeneous field environments [34].

The third procedure, taking field measurements of albedo, typically involves installing pyranometers over the test area at a height of less than half a meter, according to the ASTM E1918-06 standard [35]. This standard requires a target area of a minimum of 4 m in diameter, and the measurement should be performed in an open area [36]. Sailor et al. [37] proposed the use of a circular shield limiting the target area to 1 m and with a pyranometer installed at a height of 0.18 m. The shadows produced by the sensor and the surroundings were estimated by calculating the view factors of the mentioned surfaces. This last approach was applied in the present study.

In this article, an optimized model approach is presented for the sun drying of paddy rice to predict crop temperature and mass evaporation. The objectives of this study were to (i) develop a dynamic model to simulate the sun drying of paddy rice, (ii) determine the relationship of albedo and the solar zenith angle, and (iii) evaluate the accuracy of the model at constant and variable albedos in different environmental conditions in the Philippines.

2. Materials and Methods

2.1. Model Description

The sun drying of paddy rice was modeled based on the methodology proposed by Jain and Tiwari [5]. Figure 1 schematically shows the sun drying principle as a one-dimensional model of the thermal network with seven nodes. The layers from top to bottom are paddy rice, polyvinyl chloride

(PVC) tarpaulin, asphalt, and soil. The energy and mass balance equations were formulated as ordinary differential equations (ODEs).

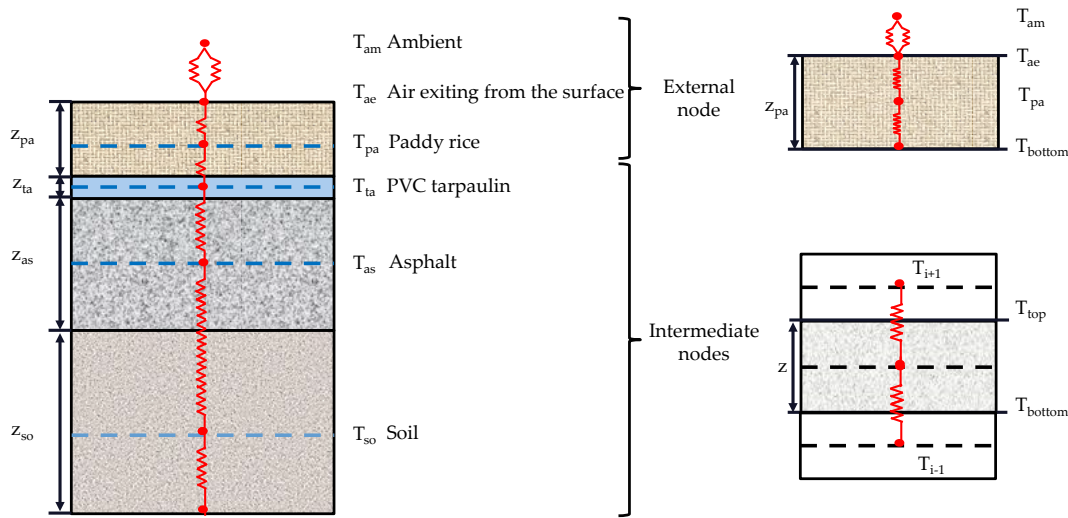


Figure 1. Thermal network of a one-dimensional model for the sun drying of paddy rice with layer thickness z and temperatures of ambient air, T_{am} , air exiting from the surface, T_{ae} , paddy rice, T_{pa} , polyvinyl chloride (PVC) tarpaulin, T_{ta} , asphalt, T_{as} , and soil, T_{so} .

2.1.1. External Node

According to the thermal network shown in Figure 1, energy balance at the external node can be expressed as:

$$m_t \cdot c_{pa} \cdot \frac{dT_{pa}}{dt} = (1 - \alpha_{pa}) \cdot G_{up} \cdot A - h_{rc,pa-ae} \cdot (T_{pa} - T_{ae}) \cdot A - Q_{ev} \cdot A - K_{pa} \cdot (T_{pa} - T_{bottom}) \cdot A \quad (1)$$

where m_t (kg) is the instantaneous mass of the paddy, α_{pa} (-) is the albedo of paddy rice, G_{up} ($W m^{-2}$) is the total solar radiation, A (m^2) is the area of the crop exposed to the sun, $h_{rc,pa-ae}$ ($W m^{-2} K^{-1}$) is the combined radiative and convective heat transfer coefficient from the paddy rice surface to the air, T_{ae} ($^{\circ}C$) is the temperature of the air exiting the paddy rice surface—henceforth called exit temperature— T_{pa} ($^{\circ}C$) is the temperature of the paddy rice, and Q_{ev} ($kJ m^{-2} s^{-1}$) is the rate of heat utilized to evaporate moisture. Q_{ev} is calculated as [38]:

$$Q_{ev} = 0.016 \cdot h_{c,pa-ae} \cdot [P_{T_{pa}} - rh_{am} \cdot P_{T_{ae}}] \quad (2)$$

where $h_{c,pa-ae}$ ($W m^{-2} K^{-1}$) is the convective heat transfer coefficient from the paddy rice surface to the air, rh_{am} (-) is the ambient relative humidity, and $P_{T_{pa}}$ and $P_{T_{ae}}$ ($N m^{-2}$) are the saturated vapor pressure at the respective temperatures. The values of P_T were extracted from the temperature range from 25 to 55 $^{\circ}C$ [39], which corresponds to the operating condition of the sun drying experiments. A 1D lookup table block built in Simulink was used to retrieve the saturated vapor pressure at the respective temperatures [40].

The energy balance of moist air above the paddy rice is calculated as:

$$h_{r,pa-ae} \cdot (T_{pa} - T_{ae}) \cdot A + Q_{ev} \cdot A = h_w \cdot (T_{ae} - T_{am}) \cdot A \quad (3)$$

where T_{am} ($^{\circ}C$) is the ambient temperature and h_w ($W m^{-2} K^{-1}$) is the convective heat transfer coefficient for wind. h_w is computed according to Duffie and Beckmann [41]:

$$h_w = 5.7 + 3.8 \cdot V_w \quad (4)$$

where V_w (m s^{-1}) is the wind velocity.

The radiative heat transfer coefficient $h_{r,pa-ae}$ is written as:

$$h_{r,pa-ae} = \varepsilon \cdot \sigma \cdot (T_{pa}^2 + T_{ae}^2) \cdot (T_{pa} + T_{ae}) \quad (5)$$

where the emissivity ε of a solid body is equal to the absorbance $(1-\alpha)$ measured at the same wavelengths according to Kirchhoff's law [32,42] and σ is the Boltzmann constant ($5.6696 \times 10^{-8} \text{ W m}^{-2} \text{ K}^{-4}$).

The calculation of the mass of paddy rice m_t during drying is done by subtracting the evaporated water from the initial mass m_0 . The evaporated mass of water m_{ev} is obtained as:

$$m_{ev} = \frac{Q_{ev}}{L_{T_{pa}}} \cdot A \cdot t \quad (6)$$

where t (h) is the time of the sampling interval and L (kJ kg^{-1}) is the latent heat of vaporization, which is calculated as [43]:

$$L = 2502.535 - 2.386 \cdot T_{pa} \quad (7)$$

2.1.2. Intermediate Nodes

The energy balance of the intermediate nodes is driven by heat conduction. Figure 1 shows the thermal network across the bottom layers, and the rate of thermal energy flow into the bottom layers is given as:

$$C_i \cdot \frac{dT_i}{dt} = K_i \cdot (T_{top} - T_i) + K_i \cdot (T_{bottom} - T_i) \quad (8)$$

where T_i corresponds to the material temperature of the respective node and C_i is the lumped thermal capacity of the material around the node, which can be calculated by knowing the specific heat capacity c_{pi} ($\text{kJ m}^{-3} \text{ K}^{-1}$), and the thickness z_i (m) of the material (9).

$$C_i = c_{pi} \cdot z_i \quad (9)$$

The thermal conductance K_i is given as:

$$K_i = \frac{\lambda_i}{\frac{1}{2} \cdot z_i} \quad (10)$$

where λ_i ($\text{kJ m}^{-2} \text{ K}^{-1}$) is the thermal conductivity of the material i (soil, asphalt, and PVC tarpaulin).

The temperatures T_{top} and T_{bottom} of the layers are known boundary conditions between the layers and are given in (11) and (12), respectively:

$$T_{top} = \frac{K_i \cdot T_i + K_{i+1} \cdot T_{i+1}}{K_i + K_{i+1}} \quad (11)$$

$$T_{bottom} = \frac{K_i \cdot T_i + K_{i-1} \cdot T_{i-1}}{K_i + K_{i-1}} \quad (12)$$

Table 1 presents the default input parameter values for the model that were found in the literature and average values that were used in the model.

Table 1. Model input parameters from the literature.

Material	Parameter	Definition	Values		
			Min	Max	Mean
Soil [4,44–47]	λ_{so}	Thermal conductivity, $\text{kJ m}^{-1} \text{K}^{-1} \text{h}^{-1}$	0.5190	5.5000	2.2598
	cp_{so}	Volumetric heat capacity, $\text{kJ m}^{-3} \text{K}^{-1}$	2000	3835	2780
Asphalt [48–50]	λ_{as}	Thermal conductivity, $\text{kJ m}^{-1} \text{K}^{-1} \text{h}^{-1}$	0.8800	1.8660	1.3020
	cp_{as}	Volumetric heat capacity, $\text{kJ m}^{-3} \text{K}^{-1}$	2188	2287	2247
PVC tarpaulin [51,52]	λ_{ta}	Thermal conductivity, $\text{kJ m}^{-1} \text{K}^{-1} \text{h}^{-1}$	0.1400	0.1500	0.1450
	cp_{ta}	Volumetric heat capacity, $\text{kJ m}^{-3} \text{K}^{-1}$	1439	1950	1694
Paddy rice [39,53,54]	λ_{pa}	Thermal conductivity, $\text{kJ m}^{-1} \text{K}^{-1} \text{h}^{-1}$	0.0895	0.1250	0.1068
	cp_{pa}	Volumetric heat capacity, $\text{kJ m}^{-3} \text{K}^{-1}$	669	891	754
	ρ_{pa}	Bulk density, kg m^{-3}	585	600	592
[10,17,21,24,30–32,55]	α_{pa}	Albedo of paddy rice, -	0.0900	0.5000	0.1957

Equations (1)–(12) were solved numerically using a variable order solver based on the numerical differentiation formulas in the ordinary differential equations (ODE15s solver Matlab/Simulink® Version 9.6 [56]). Figure 2 illustrates the flow chart procedure of the simulation.

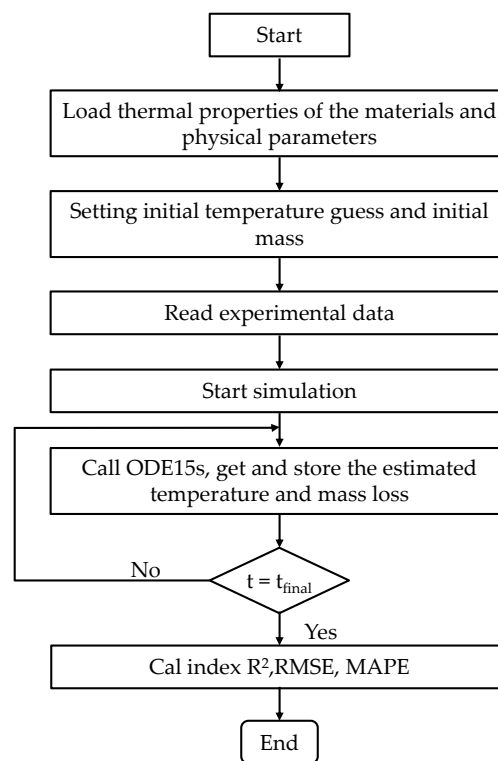


Figure 2. Flow chart of the simulation procedure.

2.2. Measurement of Albedo

To analyze the actual values for the albedo of paddy rice, experiments were performed at the International Rice Research Institute (IRRI), located in Los Baños, Laguna province, Republic of the Philippines (14°9'55" N, 121°15'3" E, 21 m a.s.l.). The albedo of paddy rice was measured according to the protocol developed by Sailor et al. [37]. In total, three sets of experiments were conducted, namely on 29 and 30 November 2012, 1 December 2012, and on 14, 15, and 25 April 2013, mostly under clear sky conditions. According to Sailor et al. [37], the measurements should be performed around

noon. The measurements carried out in this study were between 10:30 and 15:00. Figure 3 shows the setting of the sensors for the measurement of albedo.



Figure 3. Setup of the pyranometers for measuring albedo at International Rice Research Institute (IRRI) in Los Baños, Republic of the Philippines (14°9′55″ N, 121°15′37″ E).

Albedo was determined by measuring total solar radiation (direct and diffuse solar radiation) with an upward-facing pyranometer, while measuring reflected solar radiation was done with a downward-facing pyranometer (CMP11 and CMP6, Kipp and Zonen, Delftechpark, Delft, the Netherlands) from a vertical distance of 0.18 m above the paddy surface. The properties of the two pyranometers are presented in Table 2. Separate outputs for each sensor were automatically recorded using a data logger (34970A, Agilent Technologies Inc., Loveland, CO, USA). Data were logged at 1-min intervals.

Table 2. Pyranometer sensor type, properties, and specifications.

Specifications	Pyranometer Type	
	CMP6 Downward	CMP11 Upward
Field of view	180°	180°
Response time	18 s	5 s
Sensitivity	$9.05 \times 10^{-6} \text{ V W}^{-1} \text{ m}^2$	$4.96 \times 10^{-6} \text{ V W}^{-1} \text{ m}^2$
Temperature dependence of sensitivity	<4%	<1%
Spectral range	285–2800 nm	285–2800 nm
Operating temperature	−40 to + 80°C	−40 to + 80°C

The advantages of using the circular shield (Figure 3) are the reduction of the area subjected to the measurement from the minimum 4 m (standard [35]) to 1 m, the performance of the experiment without the restriction of a larger testing space, and the avoidance of the solar reflection of the surrounding surfaces on the downward pyranometer. Therefore, this setup allowed the reflected radiation to be measured over the course of the day by excluding the areas shaded by the pyranometer, its support, and the circular shield. Albedo was calculated as:

$$\alpha_{pa} = \frac{\frac{G_{down}}{G_{up}} - (F_{sensor-b} + \gamma_{diff} \cdot F_{sensor-f}) \cdot \alpha_{cs}}{F_{sensor-b} + \gamma_{diff} \cdot (F_{sensor-b} + F_{sensor-b} + F_{sensor-b})} \quad (13)$$

where α_{pa} (-) is the albedo of paddy rice, α_{cs} (-) is the albedo of the circular shield, D_{down} (W m^{-2}) is the radiation measured by the inverted pyranometer, G_{up} (W m^{-2}) is the radiation measured by

the upright pyranometer, γ_{diff} (-) is the diffuse fraction, and the view factors F between the sensor and the six surfaces are: (a) unshaded paddy sample $F_{(sensor-a)}$, (b) unshaded circular shield $F_{(sensor-b)}$, (c) pyranometer shadow $F_{(sensor-c)}$, (d) support rod shadow $F_{(sensor-d)}$, (e) crescent shade of the circular shield $F_{(sensor-e)}$, (f) and shaded part of the circular shield $F_{(sensor-f)}$, these surfaces are shown in Figure 4.



Figure 4. Top view of shadows created by the circular shield, the pyranometers and the support rod with (a) unshaded paddy rice, (b) unshaded circular shield, (c) pyranometer shadow, (d) support rod shadow, (e) crescent shade of the circular shield, and (f) shaded part of the circular shield.

The clearness index k_t was used for the calculation of γ_{diff} , according to Berrizbeitia et al. [57] and is valid for latitudes between 8.5° and 28° N.

$$\gamma_{diff} = \begin{cases} 0.98 \cdot k_t & k_t < 0.2 \\ 1.024 + 0.47 \cdot k_t - 3.62 \cdot k_t^2 + 2 \cdot k_t^3 & 0.2 < k_t < 0.77 \\ 0.16 & k_t > 0.77 \end{cases} \quad (14)$$

where k_t is the ratio of total solar radiation G_{up} and extraterrestrial radiation G_{ext} . G_{ext} is calculated as:

$$G_{ext} = 1353 \cdot \left[1 + 0.033 \cdot \cos\left(\frac{360 \cdot N}{365}\right) \right] \cdot \cos \theta \quad (15)$$

where N is the Julian day of the year and θ is the solar zenith angle, which is represented in (16):

$$\theta = \arccos(\sin \phi \cdot \sin \delta + \cos \delta \cdot \cos \phi \cdot \cos \omega) \quad (16)$$

where δ is the declination angle, ϕ is the latitude, and ω is the hour angle.

For modeling the daytime-dependent course of albedo, an approach of Zheng et al. [58] was chosen:

$$\alpha = a + b \cdot \exp^{c \cdot \theta} \quad (17)$$

where a , b , and c denote statistically estimated coefficients.

Finally, the albedo was integrated as a variable into the model for the sun drying of paddy rice.

2.3. Drying Experiments

To parametrize the model, sun drying experiments were performed on the premises of IRRI. Three batches of experiments were performed during the rainy season (October 2011 and November 2012) and dry season (May 2012 and April 2013). The paddy rice was spread out on a black PVC tarpaulin with a bulk height (z_{pa}) of 40 mm. The grains were mixed manually by using a wooden rake at 1-h intervals during daylight.

To investigate the drying performance, omega sensors (OM-EL-USB-2, Omega, Stamford, CT, United States of America) were used to monitor temperature and relative humidity over the paddy rice surface, and a separate omega sensor was used to measure ambient conditions. The precision of the temperature and relative humidity measurements of the omega logger was ± 2 and $\pm 5\%$, respectively. These sensors were placed at different positions, as shown in Figure 5. Total solar radiation was measured by a pyranometer (CMP11, Kipp & Zonen, Delftechpark, Delft, Netherlands). Pyranometers were connected to a data logger (34970A, Agilent Technologies, Inc., Loveland, CO, United States of America). Data were logged at 5-min intervals and merged with the data from the temperature/humidity loggers after each drying experiment.

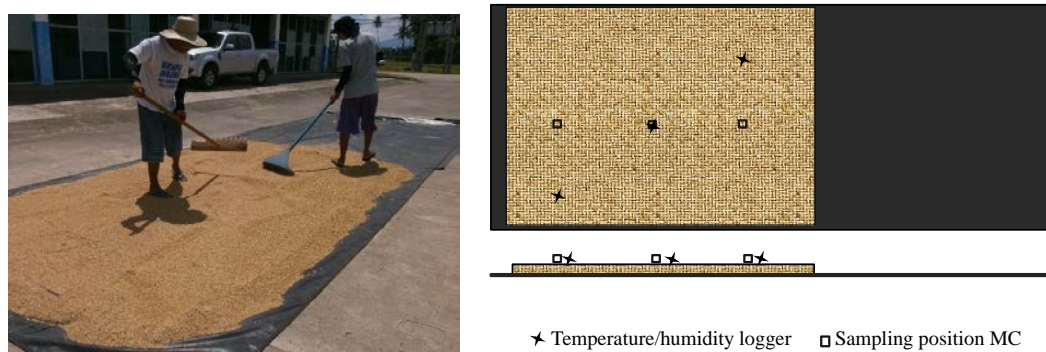


Figure 5. Manual mixing during the drying and position of measuring devices, top view and cross-section view, at IRRI in Los Baños, Republic of the Philippines (14°9′55″ N, 121°15′37″ E).

Immediately after the hourly mixing operation, a sample of about 10 g of paddy rice was taken from each of the positions shown in Figure 5. Due to the preceding mixing, a sufficient mixture of the rice layers was assumed. The samples were weighed by an electronic balance with a precision of ± 0.001 (PS-20, Voltcraft, Hirschau, Germany). Dry matter mass m_{DM} (g) was determined by drying the sample in a ventilated oven (ESP-400 Series, Blue M, White Deer, PA, United States of America) at 130 °C for 16 h [59]. The moisture content MC was calculated on dry basis.

$$MC = \frac{m_{ini}}{m_{DM}} \tag{18}$$

where m_{ini} (g) is the initial mass of the sample.

From the initial mass of paddy rice m_0 (kg) used per experimental batch (about 500 kg), the instantaneous mass m_t was calculated for one-hour intervals:

$$m_t = \frac{m_0}{(1 + MC_0)} \cdot (1 + MC_t) \tag{19}$$

where MC_0 is the initial moisture content and MC_t is the instantaneous moisture content at time t .

2.4. Statistical Analysis

2.4.1. Sensitivity Analysis

The parameters with a significant influence in the model were explored with the sensitivity analysis (SA) tool of the Matlab/Simulink® software. The SA was used to test how the variation of the input parameters affects the output behavior of the model [60,61]. Random samples of the individual parameters were generated by using a uniform distribution of its values collected from the literature. Experiments to determine the parameters’ influence on the thermal model were performed using 100 random samples of the exit temperature T_{ae} and the instantaneous mass m_t . Then, a Monte Carlo

evaluation was carried out on T_{ae} and m_t . Finally, the standardized regression coefficient (R) was calculated between all the parameters under the partial derivatives by using (20).

$$R = b_x \cdot \frac{\sigma_x}{\sigma_y} \tag{20}$$

where b_x is the regression coefficient, σ_x is the standard deviation of the corresponding sample, and σ_y is the standard deviation of the partial derivatives. A tornado plot shows the results of the SA analysis [61].

2.4.2. Albedo Model

Matlab Version 9.6 software [62] was used for fitting the experimental values of paddy rice albedo by applying the non-linear least squares method to the two proposed models. The model with the highest coefficient of determination (R^2) and the lowest root mean square error ($RMSE$) was selected.

Code developed in Matlab Version 9.6 software was used to assess model performance at constant and variable albedos. R^2 , $RMSE$, and mean absolute percentage error ($MAPE$) were used to indicate the accuracy of the prediction.

3. Results

3.1. Measurements of Albedo

Figure 6 exemplarily shows the course of solar radiation, the solar zenith angle, and the albedo of paddy rice for the rainy season (19 November 2012) and for the dry season (15 April 2013). Fluctuations in albedo were encountered when clouds passed through the experimental area. A higher albedo of paddy rice was observed in the rainy season than in the dry season, with values of 0.29 and 0.25, respectively, at noon. Nevertheless, the obtained values were higher than the mean value calculated from literature data (Table 1).

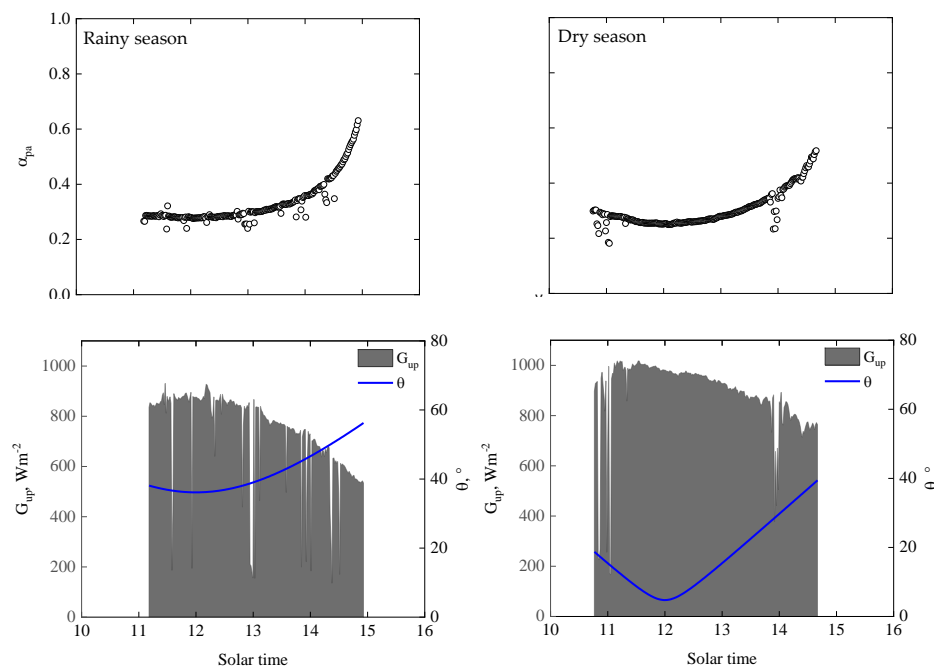


Figure 6. Total solar radiation G_{up} , zenith angle θ , and albedo of paddy rice α during the rainy season (19 November 2012) and the dry season (15 April 2013) at IRRI in Los Baños, Republic of the Philippines (14°9'55" N, 121°15'37" E).

Based on Equation (17), the albedo can be modeled for the course of the day as a function of the solar zenith angle:

$$\alpha = 0.2704 + 1.816 \cdot 10^{-5} \cdot e^{0.1761 \cdot \theta} \tag{21}$$

With an R^2 of 0.7880 and $RSME$ of 0.0299.

3.2. Parameters' Influence

Figure 7 shows the tornado plot in which parameters are ranked by influence. An example of these results is shown for one batch during the rainy season (4 June 2012). According to the sensitivity analysis, the albedo has the most significant influence, and the other parameters have little effect. This means that at a higher albedo, lower air temperatures are expected. In the case of the instantaneous mass of paddy rice during drying, albedo is also the main parameter of influence, and the other parameters have less impact. Higher albedo values result in lower energy. Therefore, using a constant albedo value in the model may result in the over/underestimation of paddy rice temperature, and consequently, drying rate. Similar results were found for all the experiments and they showed a significant influence of albedo, with a correlation R ranging from -0.81 to -0.67 for the estimation of the exit temperature and from 0.92 to 0.98 for the instantaneous mass during drying.

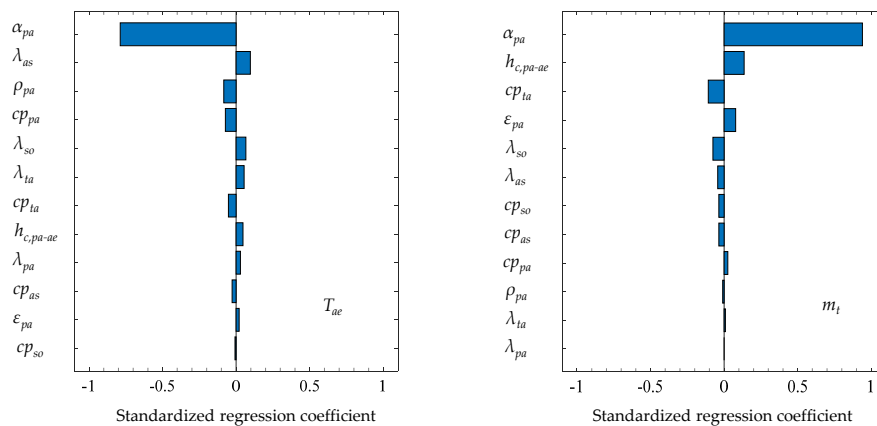


Figure 7. Standardized regression coefficient R from the sensitivity analysis of exit temperature (T_{ae}) and instantaneous mass (m_t) of the thermal sun drying model on 4 June 2012 (paddy rice: α_{pa} —albedo, d_{pa} —density, cp_{pa} —volumetric heat capacity, λ_{pa} —thermal conductivity; PVC tarpaulin: cp_{ta} —volumetric heat capacity, λ_{pvc} —thermal conductivity; Asphalt: cp_{as} —volumetric heat capacity, λ_{as} —thermal conductivity; Soil: cp_{so} —volumetric heat capacity, λ_{so} —thermal conductivity, h_c heat transfer coefficient from the paddy rice to the air).

3.3. Meteorological Conditions during the Drying Experiments

Figure 8 shows an example of the weather conditions during the sun drying of paddy rice during the rainy season (19 October 2011) and dry season (22 May 2012). Weather data collected for the other experiments were similar to the corresponding season. The sun drying conditions in the dry season were characterized by an ambient relative humidity of about 40%; the ambient temperature ranged from 30 to 38 °C, and solar irradiation ranged from 4 to 5 kWh m⁻² d⁻¹. Compared with conditions in the rainy season, higher values of relative humidity of about 60%, lower temperatures of about 30 °C, and lower solar radiation values of about 3 kWh m⁻² d⁻¹ were expected, primarily due to cloudiness. In both seasons, relative humidity reached values of over 80%, with temperatures of around 25 °C during the night. Furthermore, a higher variability of solar radiation is typically experienced during the rainy season.

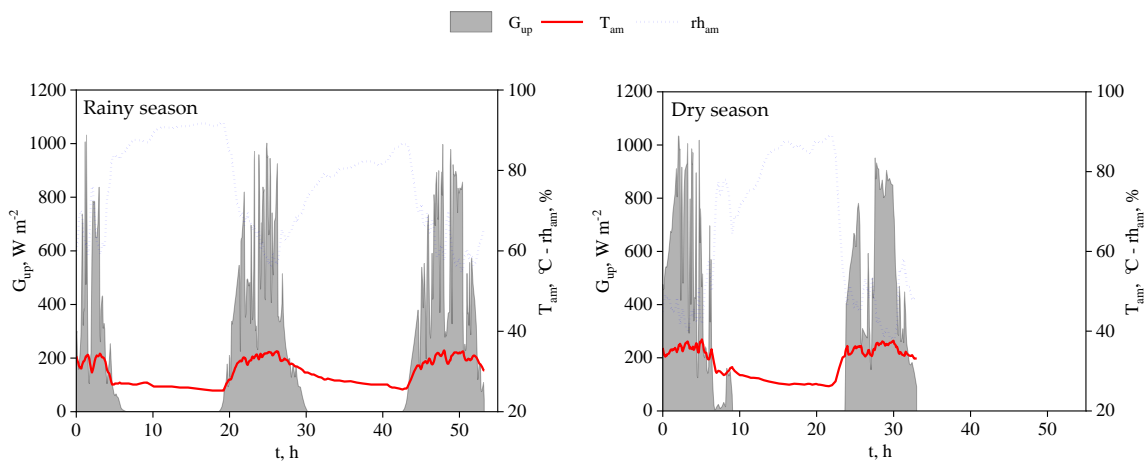


Figure 8. Total solar radiation G_{up} , ambient temperature T_{am} , and relative humidity rh_{am} during an exemplary drying batch in the dry season (22 May 2012) and the rainy season (19 October 2012) at IRRI in Los Baños, Republic of the Philippines (14°9'55" N, 121°15'37" E).

3.4. Estimation of Temperatures

Figure 9 shows the simulated and the experimental temperatures over the paddy rice during the dry and rainy seasons. Due to lower cloudiness, a higher temperature was expected during the dry season compared to the rainy season. Nevertheless, the simulated exit temperature in the rainy season showed higher variation at night compared with the experimental temperature over the paddy rice. This variation was not observed during the dry season. During the course of the day, the simulated temperature over the paddy rice for the rainy season showed higher values compared to the dry season. It could be as much as 5 °C higher than the experimental value. Therefore, we can assume that the dynamic sun drying model provides an accurate estimation of the crop temperature.

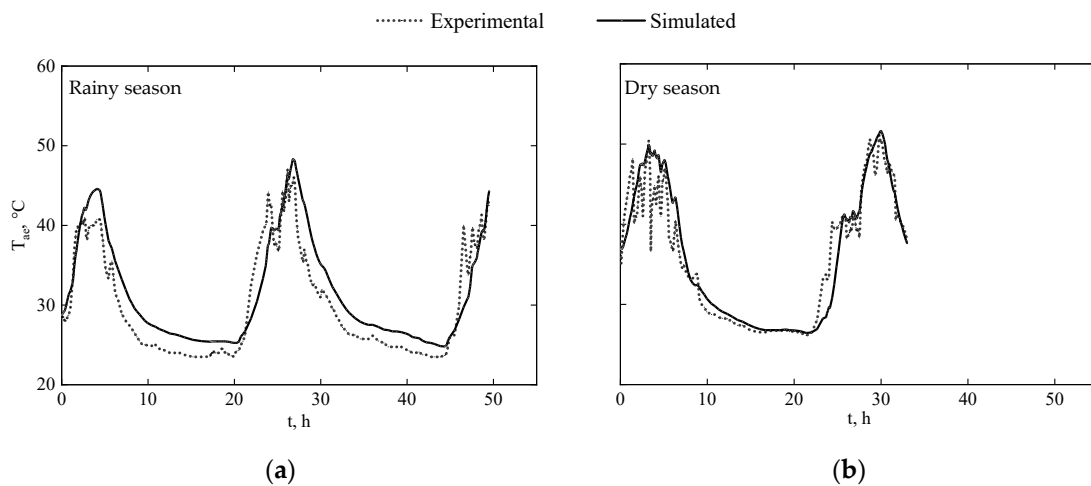


Figure 9. The experimental and simulated exit temperature T_{ae} surface during the rainy season (22 November 2012) (a) and the dry season (4 June 2012) (b).

Figure 10 provides the simulated temperatures of the soil T_{so} , asphalt T_{as} , PVC tarpaulin T_{ta} , paddy rice T_{pa} , and air exiting the paddy rice surface T_{ae} . It can be seen that the paddy rice temperature reached temperatures higher than 50 °C during the dry season. While temperatures reached almost 50 °C or lower during the rainy season.

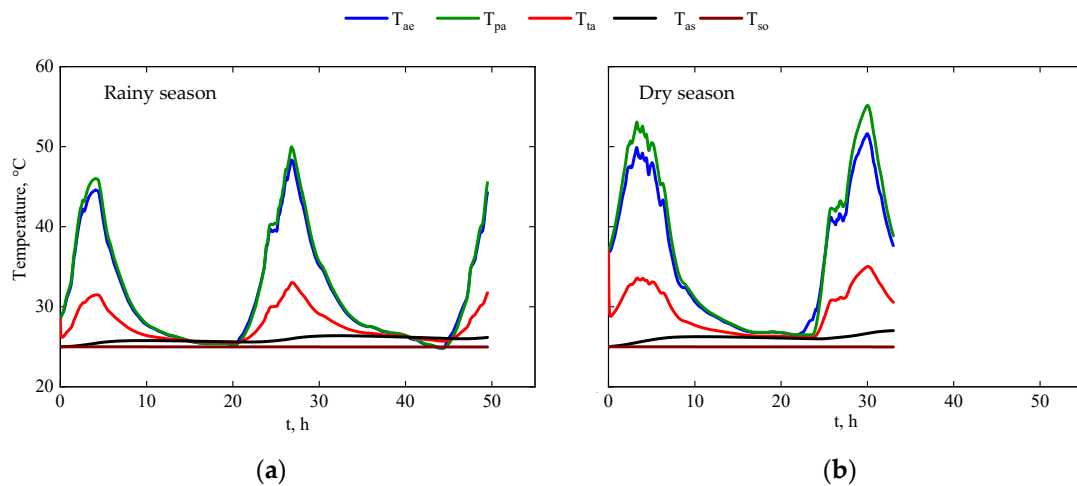


Figure 10. The simulated temperatures during the rainy season (22 November 2011) (a) and the dry season (4 June 2012) (b); temperature: air exiting the paddy rice surface T_{ac} , paddy rice T_{pa} , PVC tarpaulin T_{ta} , asphalt T_{as} , and soil T_{so} .

3.5. Estimation of Moisture Content during Drying

Figure 11 shows a comparison of the simulated and the experimental moisture content of paddy rice during sun drying. The drying curves for the rainy season and the dry season are shown exemplarily. It was observed that the moisture content decreased continuously with drying time. The absence of connection lines in Figure 11 indicates night periods. The MC of the paddy rice for all the experiments decreased from the range of 0.18 to 0.38 to about 0.16 within 3.5 to 76.7 h (Table 3). Although there were slight discrepancies between the simulated and the experimental moisture content, the results obtained by the sun drying model are in good agreement with the experimental data, as the MAPE values were below 2%.

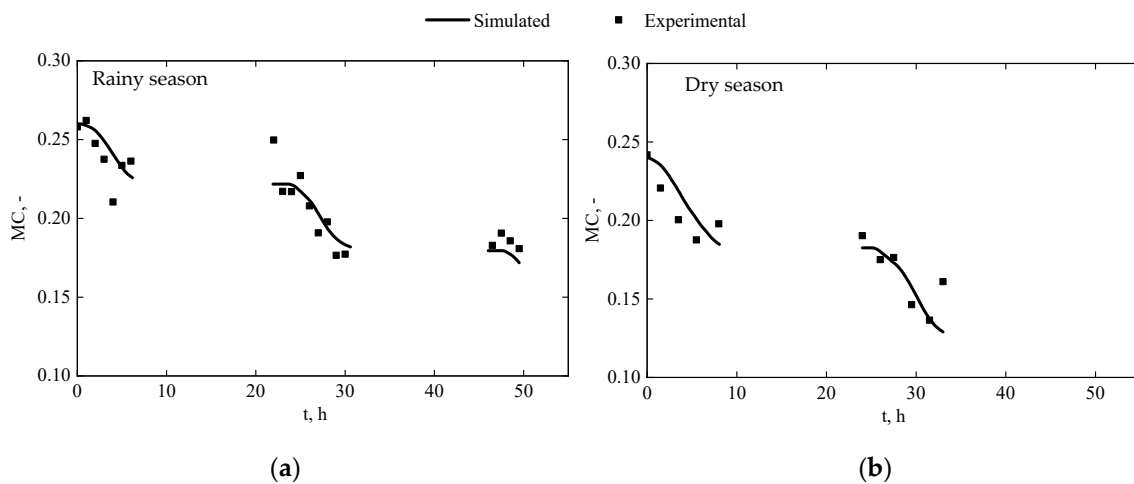


Figure 11. Experimental and simulated moisture content MC during the rainy season (22 November 2012) (a) and dry season (4 June 2012) (b).

Table 3. Coefficient of determination R^2 of air temperatures T_{ae} and instantaneous mass m_t at a constant albedo (C) of $\alpha_{pa} = 0.1957$ and variable (V) albedo α_{pa} .

Season	Date	MC _{ini}	Drying Time	Albedo	T_{ae}	m_t
		–	h		R^2	R^2
Rainy	12.10.2011	0.3363	52.0	C	0.6396	0.2029
				V	0.6114	0.2182
	19.10.2011	0.2490	52.3	C	0.8363	0.8952
				V	0.8161	0.9049
	25.10.2011	0.2909	76.7	C	0.6562	0.8524
				V	0.6753	0.8682
	14.11.2012	0.3810	43.0	C	0.8199	0.8611
				V	0.8729	0.8160
	19.11.2012	0.3530	54.4	C	0.8335	0.9021
				V	0.7427	0.9012
	22.11.2012	0.2578	49.5	C	0.8777	0.8491
				V	0.8328	0.8352
Dry	22.05.2012	0.2431	26.0	C	0.8012	0.6700
				V	0.7234	0.6722
	29.05.2012	0.2441	30.0	C	0.8012	0.7000
				V	0.8135	0.7340
	04.06.2012	0.2427	33.0	C	0.8725	0.8426
				V	0.8818	0.8490
	09.04.2013	0.1897	29.5	C	0.8062	0.9328
				V	0.7471	0.9405
	11.04.2013	0.1680	3.5	C	0.9246	0.9847
				V	0.9304	0.9859
	16.04.2013	0.2589	29.5	C	0.7682	0.9692
				V	0.7611	0.9571

3.6. Accuracy of the Model of Variable vs. Constant Albedo

To assess the model with constant or variable albedo values, *RMSE*, *MAPE*, and R^2 were used for T_{ae} and m_t . Figure 12 shows that for T_{ae} , the *RMSE* and *MAPE* are lower in most cases for variable albedo in both seasons, with values for *RMSE* ranging from 3 to 7.5 and below 10% for *MAPE*, while R^2 shows a minor increment for variable albedo compared to the constant values. Interestingly for the instantaneous mass, *RMSE* and *MAPE* show a more significant improvement of the model outputs when a variable albedo is used. Furthermore, the R^2 shows slightly higher values of the model with variable albedo compared to the constant albedo (Table 3). Overall, these results indicate that there is a strong influence of variable albedo in the developed sun drying model.

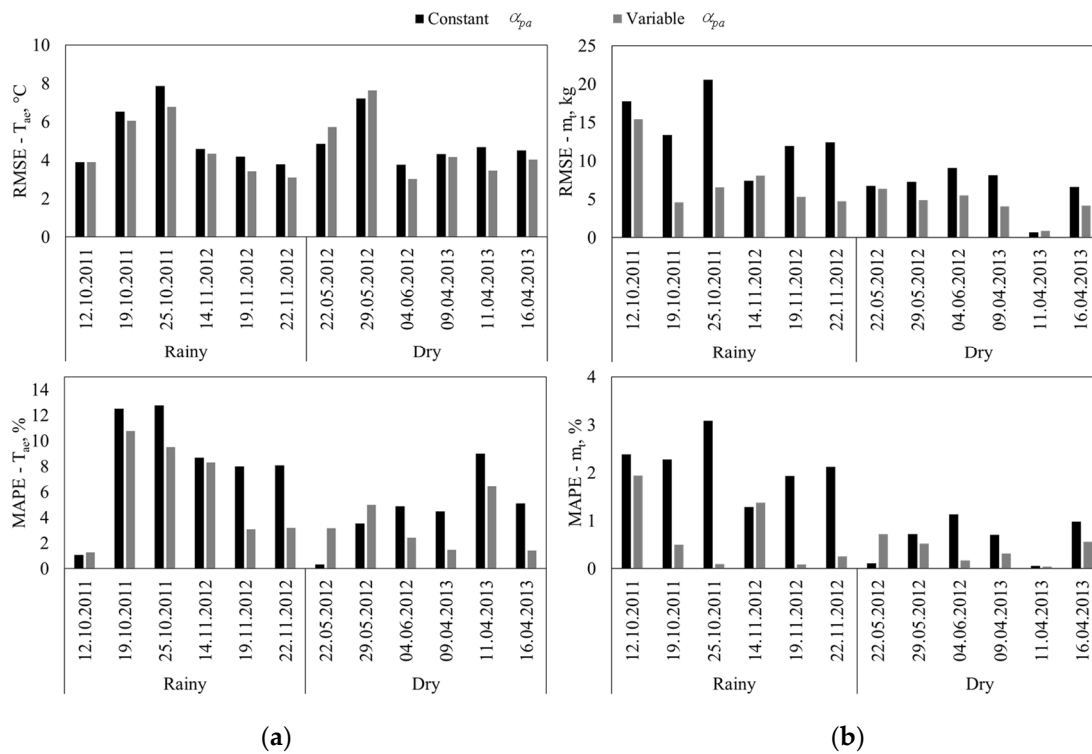


Figure 12. The lowest root mean square error RMSE and the mean absolute percentage error MAPE for constant and variable albedo α_{pa} for exit temperature T_{ae} (a) and for predicted instantaneous mass m_t (b) during the rainy season and dry season.

4. Discussion

In previous studies on simulating sun drying, constant albedo values have been used, and the energy exchange within the layers under the paddy rice has been neglected. Moreover, steady state rather than transient state conditions are commonly assumed for solving equations in thermal analysis. Thus, temporary heat and mass transfer analyses were explored and presented in this paper.

In reviewing the literature, Sailor et al.'s [37] approach resulted in a practical procedure to assess the measurement of albedo. We obtained an albedo value of around 0.25–0.28, corresponding to the period from 11:00 to 13:00 (Figure 6). This albedo value is higher than the values reported by other studies such as Arninze et al. [21] and Bala [32], who proposed an albedo of 0.16 for brown rice. On the other hand, the presented range found in this study lies within the range provided by Arya [17], who proposed values for wheat and rice in a range from 0.18 to 0.25. The albedo of paddy rice was shown to correlate with solar zenith angle, showing an R^2 of 0.7880 and $RSME$ of 0.0299. Hence, the solar zenith angle should be used for the parametrization of the albedo of paddy rice in modeling schemes in solar drying applications [10,58].

The results of the sun drying model show that when a variable, daytime-dependent albedo was applied, most of the RMSE and MAPE values were smaller for the estimation of the exit temperature and for the instantaneous mass than when using a constant albedo. Another important finding is that RMSE and MAPE with variable albedos are much lower for the instantaneous mass than for the exit temperature, showing that the model provides a better estimation of instantaneous mass. This was already observed from the sensitivity analysis, where albedo showed higher standardized regression values for the instantaneous mass than for the exit temperature.

5. Conclusions

A clear understanding of the incident solar radiation is essential for the effective use of the solar energy.

Albedo, i.e., the solar energy reflected from a surface, is an important component of the energy balance in the solar drying process. This study results suggest that the albedo of the drying product should not be regarded as a constant value, but that the day-dependent variation should be taken into account when estimating energy balances, and thus the course of the moisture content during drying. Furthermore, the development of a mathematical model serves to improve understanding of the dynamic behavior of paddy rice during sun drying. Thus, the modeling of the sun drying of paddy rice can support management decisions for the proper handling of paddy rice.

Author Contributions: Conceptualization, A.S.-R., V.T.-T., and J.M.; data curation, A.S.-R.; formal analysis, A.S.-R., V.T.-T., and J.M.; funding acquisition, A.S.-R. and J.M.; investigation, A.S.-R.; methodology, A.S.-R. and J.M.; resources, A.S.-R. and J.M.; software, A.S.-R. and V.T.-T.; supervision, J.M.; validation, A.S.-R., V.T.-T., and J.M.; visualization, A.S.-R.; writing—original draft preparation, A.S.-R.; writing—review and editing, A.S.-R. and J.M. All authors have read and agreed to the published version of the manuscript.

Funding: This research was supported by the scholarships awarded by the Carl Zeiss Foundation (Stuttgart, Germany), Fiat Panis Foundation (Ulm, Germany), and Global Rice Science Scholarships—IRRI (Los Baños, Republic of Philippines).

Acknowledgments: We wish to express our appreciation to Marcus Nagle for this academic supervision and Sabine Nugent for language editing, and to the kind and supportive staff members at IRRI, specifically Martin Gummert, Eduardo Secretario, and Elenita Suñaz.

Conflicts of Interest: The authors declare no conflict of interest.

References

- Bhattacharya, K.R. 3-Milling Quality of Rice. In *Rice Quality*; Bhattacharya, K.R., Ed.; Woodhead Publishing: Cambridge, UK, 2013; pp. 61–99. [[CrossRef](#)]
- Verma, D.K.; Srivastav, P.P.; Nadaf, A.B. Nutritional Quality Evaluation of Different Rice Cultivars. In *Agronomic Rice Practices and Postharvest Processing: Production and Quality Improvement*; Apple Academic Press Inc.: Oakville, Canada, 2018; pp. 299–348.
- Salvatierra-Rojas, A.; Nagle, M.; Gummert, M.; de Bruin, T.; Müller, J. Development of an inflatable solar dryer for improved postharvest handling of paddy rice in humid climates. *Int. J. Agric. Biol. Eng.* **2017**, *10*, 269–282. [[CrossRef](#)]
- Meas, P.; Paterson, A.H.J.; Cleland, D.J.; Bronlund, J.E.; Mawson, A.J.; Hardacre, A.; Rickman, J.F. A mathematical model of solar drying of rice. *Int. J. Food Eng.* **2012**, *8*. [[CrossRef](#)]
- Jain, D.; Tiwari, G.N. Thermal aspects of open sun drying of various crops. *Energy* **2003**, *28*, 37–54. [[CrossRef](#)]
- Hande, A.R.; Swami, S.B.; Thakor, N.J. Open-Air Sun Drying of Kokum (*Garcinia indica*) Rind and Its Quality Evaluation. *Agric. Res.* **2016**, *5*, 373–383. [[CrossRef](#)]
- Anwar, S.I.; Tiwari, G.N. Evaluation of convective heat transfer coefficient in crop drying under open sun drying conditions. *Energy Convers. Manag.* **2001**, *42*, 627–637. [[CrossRef](#)]
- Kumar, M.; Khatak, P.; Sahdev, R.K.; Prakash, O. The effect of open sun and indoor forced convection on heat transfer coefficients for the drying of papad. *J. Energy S. Afr.* **2011**, *22*, 40–46. [[CrossRef](#)]
- Togrul, I.T. Determination of convective heat transfer coefficient of various crops under open sun drying conditions. *Int. Commun. Heat Mass Transf.* **2003**, *30*, 285–294. [[CrossRef](#)]
- Tsai, J.L.; Tsuang, B.J.; Lu, P.S.; Yao, M.H.; Shen, Y. Surface energy components and land characteristics of a rice paddy. *J. Appl. Meteorol. Climatol.* **2007**, *46*, 1879–1900. [[CrossRef](#)]
- Chu, S. Albedo. In *Solar and Infrared Radiation Measurements*, 2nd ed.; CRC Press: Boca Raton, FL, USA, 2012; pp. 193–204.
- Chappell, A.; Webb, N.P. Using albedo to reform wind erosion modelling, mapping and monitoring. *Aeolian Res.* **2016**, *23*, 63–78. [[CrossRef](#)]
- Cierniewski, J.; Ceglarek, J.; Kaźmierowski, C. Estimating the diurnal blue-sky albedo of soils with given roughness using their laboratory reflectance spectra. *J. Quant. Spectrosc. Radiat. Transf.* **2018**, *217*, 213–223. [[CrossRef](#)]
- Jacobs, A.F.G.; Van Pul, W.A.J. Seasonal changes in the albedo of a maize crop during two seasons. *Agric. For. Meteorol.* **1990**, *49*, 351–360. [[CrossRef](#)]

15. Favero, A.; Sohngen, B.; Huang, Y.; Jin, Y. Global cost estimates of forest climate mitigation with albedo: A new integrative policy approach. *Environ. Res. Lett.* **2018**, *13*. [[CrossRef](#)]
16. Nkemdirim, L.C. A Note on the Albedo of Surfaces. *J. Appl. Meteorol.* **1972**, *11*, 867–874. [[CrossRef](#)]
17. Arya, P.S. Radiation Balance Near the Surface. In *Introduction to Micrometeorology*, 2nd ed.; Holton, J.R., Ed.; Elsevier Science Publishing Co Inc.: San Diego, CA, USA, 2001; Volume 79, pp. 28–45.
18. Ineichen, P.; Guisan, O.; Perez, R. Ground-reflected radiation and albedo. *Sol. Energy* **1990**, *44*, 207–214. [[CrossRef](#)]
19. Wang, Z.; Barlage, M.; Zeng, X.; Dickinson, R.E.; Schaaf, C.B. The solar zenith angle dependence of desert albedo. *Geophys. Res. Lett.* **2005**, *32*, 1–4. [[CrossRef](#)]
20. Yang, F.; Mitchell, K.; Hou, Y.-T.; Dai, Y.; Zeng, X.; Wang, Z.; Liang, X.-Z. Dependence of Land Surface Albedo on Solar Zenith Angle: Observations and Model Parameterization. *J. Appl. Meteorol. Climatol.* **2008**, *47*, 2963–2982. [[CrossRef](#)]
21. Arinze, E.A.; Schoenau, G.J.; Bigsby, F.W. Determination of solar energy absorption and thermal radiative properties of some agricultural products. *Trans. Am. Soc. Agric. Eng.* **1987**, *30*, 259–265. [[CrossRef](#)]
22. Murata, Y.; Miyasaka, A.; Munakata, K.; Akita, S. On the Solar Energy Balance of Rice Population in Relation to the Growth Stage. *Jpn. J. Crop Sci.* **1968**, *37*, 685–691. [[CrossRef](#)]
23. Iqbal, M. Ground Albedo. In *An Introduction To Solar Radiation*; Academic Press: Toronto, Canada, 1983; pp. 281–293.
24. Higuchi, A.; Kondoh, A.; Kishi, S. Relationship among the surface albedo, spectral reflectance of canopy, and evaporative fraction at grassland and paddy field. *Adv. Space Res.* **2000**, *26*, 1043–1046. [[CrossRef](#)]
25. Iwamoto, A.; Urano, S.I.; Aragaki, M. Water Budget and Estimation of Net Water Requirement for Paddy Field in the Zambezi River Flood Plain, Zambia. *J. Agric. Meteorol.* **1998**, *54*, 125–131. [[CrossRef](#)]
26. Nakagawa, K.; Ooi, Y. The surface albedo distribution and its seasonal change over the Nagaoka area, Niigata Prefecture, central Japan, estimated with Landsat/MSS data. *Geogr. Rev. Jpn. Ser. A* **1992**, *65*, 769–790. [[CrossRef](#)]
27. Susaki, J.; Yasuoka, Y.; Kajiwara, K.; Honda, Y.; Hara, K. Validation of MODIS albedo products of paddy fields in Japan. *IEEE Trans. Geosci. Remote Sens.* **2007**, *45*, 206–217. [[CrossRef](#)]
28. Linacre, E. Estimating Climate Data. In *Climate Data and Resources: A Reference and Guide*; Routledge: London, UK, 1992; pp. 54–91.
29. Maruyama, A.; Kuwagata, T.; Ohba, K.; Maki, T. Dependence of solar radiation transport in rice canopies on developmental stage. *Jpn. Agric. Res. Q.* **2007**, *41*, 39–45. [[CrossRef](#)]
30. Gao, Z.; Bian, L.; Zhou, X. Measurements of turbulent transfer in the near-surface layer over a rice paddy in China. *J. Geophys. Res. Atmos.* **2003**, *108*, ACL 6-1–ACL 6-13. [[CrossRef](#)]
31. Belessiotis, V.; Delyannis, E. Solar drying. *Solar Energy* **2011**, *85*, 1665–1691. [[CrossRef](#)]
32. Bala, B.K. Fluid Mechanics and Heat Transfer in Solar Drying. In *Solar Drying Systems: Simulations and Optimization*; Agrotech Publishing Academy: Delhi, India, 1998; pp. 49–86.
33. Berdahl, P.; Bretz, S.E. Preliminary survey of the solar reflectance of cool roofing materials. *Energy Build.* **1997**, *25*, 149–158. [[CrossRef](#)]
34. Cao, C.; Lee, X.; Muhlhausen, J.; Bonneau, L.; Xu, J. Measuring landscape albedo using unmanned aerial vehicles. *Remote Sens.* **2018**, *10*, 1812. [[CrossRef](#)]
35. ASTM. *E1918-06-Standard Test Method for Measuring Solar Reflectance of Horizontal and Low-Sloped Surfaces in the Field*; ASTM International: West Conshohocken, PA, USA, 2006.
36. Qin, Y.; He, H. A new simplified method for measuring the albedo of limited extent targets. *Solar Energy* **2017**, *157*, 1047–1055. [[CrossRef](#)]
37. Sailor, D.J.; Resh, K.; Segura, D. Field measurement of albedo for limited extent test surfaces. *Solar Energy* **2006**, *80*, 589–599. [[CrossRef](#)]
38. Das, T.; Bora, G. Greenhouse Solar Thermal Application. In *Handbook of Research on Solar Energy Systems and Technologies*; Anwar, S., Ed.; IGI Global: Hershey, PA, USA, 2013; pp. 462–479.
39. Brooker, D.B.; Bakker-Arkema, F.W.; Hall, C.W. Grain structure, composition and properties. In *Drying and Storage Of Grains and Oilseeds*; Springer Science & Business Media: New York, NY, USA, 1992; pp. 19–26.
40. MathWorks. PS Lookup Table (1D). Available online: <https://de.mathworks.com/help/phymod/simscape/ref/pslookuptable1d.html> (accessed on 28 June 2020).

41. Duffie, J.A.; Beckman, W.A. Selected Heat Transfer Topics. In *Solar Engineering of Thermal Processes*, 4th ed.; John Wiley & Sons Inc.: Hoboken, NJ, USA, 2013; pp. 138–172.
42. Palmer, J. The Measurement of Transmission, Absorption, Emission and Reflection. In *Handbook of Optics: Devices, Measurements, and Properties*, 2nd ed.; Bass, M., Ed.; McGraw-Hill Inc.: New York, NY, USA, 1995; pp. 25.1–25.25.
43. ASABE. Psychrometric Data. ASAE D271.2 APR1979, R2014. Available online: <http://elibrary.asabe.org/abstract.asp?aid=32006&t=2> (accessed on 3 June 2020).
44. Campbell, G.S. Soil Temperature and Heat Flow. In *Soil Physics with BASIC: Transport Models for Soil-Plant Systems*; Elsevier Science: Amsterdam, The Netherlands, 1985; Volume 14, pp. 26–39.
45. Takakura, T.; Fang, W. Heat Balance of Bare Ground. In *Climate Under Cover*, 2nd ed.; Springer Science & Business Media: New York, NY, USA, 2002; pp. 45–64.
46. Campbell, G.S.; Norman, J. Radiation Fluxes in Natural Environments. In *An Introduction to Environmental Biophysics*, 2nd ed.; Springer: New York, NY, USA, 2012; pp. 167–184.
47. Sodha, M.S.; Bansal, P.K.; Dang, A.; Sharma, S.B. Open Sun Drying: An Analytical Study. *Dry. Technol.* **1985**, *3*, 517–527. [[CrossRef](#)]
48. Bai, B.C.; Park, D.W.; Vo, H.V.; Dessouky, S.; Im, J.S. Thermal Properties of Asphalt Mixtures Modified with Conductive Fillers. *J. Nanomater.* **2015**, *2015*. [[CrossRef](#)]
49. Sreedhar, S.; Biligiri, K.P. Development of pavement temperature predictive models using thermophysical properties to assess urban climates in the built environment. *Sustain. Cities Soc.* **2016**, *22*, 78–85. [[CrossRef](#)]
50. Hassn, A.; Chiarelli, A.; Dawson, A.; Garcia, A. Thermal properties of asphalt pavements under dry and wet conditions. *Mater. Des.* **2016**, *91*, 432–439. [[CrossRef](#)]
51. Subramanian, M.N. Polymers. In *Polymer Blends and Composites: Chemistry and Technology*; John Wiley & Sons Inc.: Beverly, MA, USA, 2017; pp. 7–55.
52. Crawford, R.J. General Properties of Plastics. In *Plastics Engineering*, 2nd ed.; Pergamon Press: Oxford, UK, 1987; pp. 1–40.
53. Meas, P. Mathematical Modelling and Improvement of Operating Practices of Sun Drying of Rice: A Thesis Presented in Partial Fulfilment of the Requirements for the Degree of Doctor of Philosophy [i.e. Philosophy] at Massey University. Ph.D. Thesis, Massey University, Wellington, New Zealand, 2008.
54. Iguaz, A.; San Martín, M.B.; Arroqui, C.; Fernández, T.; Maté, J.I.; Vírveda, P. Thermophysical properties of medium grain rough rice (LIDO cultivar) at medium and low temperatures. *Eur. Food Res. Technol.* **2003**, *217*, 224–229. [[CrossRef](#)]
55. Garratt, J.R. Energy Fluxes at the Land Surface. In *The Atmospheric Boundary Layer*; Houghton, J., Rycroft, M., Dessler, A., Eds.; Cambridge University Press: Cambridge, UK, 1994; pp. 115–144.
56. MathWorks. Ordinary Differential Equations. Available online: https://de.mathworks.com/help/matlab/ordinary-differential-equations.html?s_tid=CRUX_lftnav (accessed on 2 March 2020).
57. Berrizbeitia, S.E.; Gago, E.J.; Muneer, T. Empirical models for the estimation of solar sky-diffuse radiation. A review and experimental analysis. *Energies* **2020**, *13*, 701. [[CrossRef](#)]
58. Zheng, Z.; Wei, Z.; Wen, Z.; Dong, W.; Li, Z.; Wen, X.; Zhu, X.; Ji, D.; Chen, C.; Yan, D. Inclusion of Solar Elevation Angle in Land Surface Albedo Parameterization Over Bare Soil Surface. *J. Adv. Model. Earth Syst.* **2017**, *9*, 3069–3081. [[CrossRef](#)]
59. RKB. Measuring rice moisture content. Available online: <http://www.knowledgebank.irri.org/training/fact-sheets/postharvest-management/rice-quality-fact-sheet-category/item/measuring-rice-moisture-content-fact-sheet> (accessed on 1 February 2020).
60. Saltelli, A.; Ratto, M.; Andres, T.; Campolongo, F.; Cariboni, J.; Gatelli, D.; Saisana, M.; Tarantola, S. *Global Sensitivity Analysis. The Primer*; John Wiley & Sons: Hoboken, NJ, USA, 2008; pp. 1–292. [[CrossRef](#)]
61. MathWorks. Sensitivity Analysis. Available online: <https://de.mathworks.com/help/slido/sensitivity-analysis.html> (accessed on 2 March 2020).
62. The MathWorks Inc. *MATLAB*, version 9.6.0 (R2019a); The MathWorks Inc.: Natick, MA, USA, 2019.

